Numerical Modelling of Thermal Effects in Elastohydrodynamic Lubrication Solvers

R Fairlie[a]* C.E.Goodyer,[a] M.Berzins,[a] and L.E.Scales,[b]

[a]Computational PDEs Unit, School of Computing, University of Leeds, Leeds, UK

[b]Shell Global Solutions, Chester, UK

The numerical modelling of thermal effects in elastohydrodynamic lubrication solvers is addressed by extending the code of the authors. This code is used to investigate the important effect of shear upon the temperature profiles for both a steady state and a transient line reversal example and also for a steady state point contact problem. Additional equations for the modelling of mean and surface temperatures within an elastohydrodynamic lubrication contact are described and are added into the existing multigrid driven solver. Temperature profiles in steady line and point contact cases are presented and used to demonstrate that even small amounts of shear produce temperatures in excess of those in the pure rolling case.

1. Introduction

Within an elastohydrodynamically lubricated (EHL) contact the temperature of both the entrained fluid and the contact surfaces can vary dramatically. In the pure rolling case temperature rises of only a matter of degrees may be expected, however when shear occurs the temperature may rise in severe cases by in excess of a hundred degrees [1]. Fluid temperature plays a direct role in governing the density and viscosity of a fluid, which in turn affects the pressure profile and surface deformation across the contact. Clearly, then, with temperature fluctuations of this magnitude occurring it is important to include thermal effects in EHL models.

These thermal effects have been extensively studied for many years since the initial theoretical work by Crook [2] in 1961, with numerical methods for the thermal solutions in line contacts developed in the 1960's by Sternlicht [3], Cheng and Sternlicht [4], Cheng [5] and by Dowson and Whitaker [6]. Recent papers, for example, those by Lee *et al [7], [8], by Kim* et al [9,10] and by Kazama et al [11] have utilised the multigrid techniques applied to EHL problems by Venner and Lubrecht [12] to solve both line and point contact cases.

In this paper the transient EHL model developed in the CPDE Unit at Leeds, [13,14] using the multigrid techniques applied to EHL problems by Venner and Lubrecht [12] is extended to include thermal effects [16]. This involves extensions to the non-Newtonian fluid model [16] governing the density and viscosity and introducing three additional equations to the code, one for mean temperature and one for each of the two contact surfaces. Inclusion of these into the equation set for the line contact case will be discussed along with the solution method. An extension to the point contact case is also described.

Results are presented and discussed for an essentially steady state line contact showing the thermal effects at both pure rolling and at several shear rates, followed by thermal profiles in a line contact reversal problem, again for both pure rolling and varying shear rates. A thermal point contact solution will then be presented.

2. Notation

Dimensional Values

C_p	spec heat capacity $(Jkg^{-1}K^{-1})$
$C_p : a$	spec heat capacity of roller A $(Jkg^{-1}K^{-1})$

*The authors would like to thank Shell Global Solutions and EPSRC for funding this work

$C_p : b$	spec heat capacity of roller B ($Jkg^{-1}K^{-1}$)
p	pressure (Pa)
h	film thickness (m)
ρ	density (Nm^{-1})
ρ_a, ρ_b	density of roller A/B (Nm^{-1})
u_a, u_b	velocity of roller A/B (ms^{-1})
u_e	entrainment velocity (ms^{-1})
η	viscosity (Pas)
θ	temperature (K)
x	distance (m)
t	time (s)
μ	Dowson-Higginson mu parameter (Pa^{-1})
ν	Dowson-Higginson nu parameter (Pa^{-1})
$\beta_{e;0}$	thermal expansion coefficient (K^{-1})
κ_e	pressure coeff of thermal expansion (Pa^{-1})
θ_0	reference temperature (K)
b	Hertzian radius (m)
p_h	maximum Hertzian pressure (Pa)
R	reduced radius (m)
ρ_0	standard density (Nm^{-1})
η_0	standard viscosity (Pas)
α_0	pressure coefficient of viscosity (Pa^{-1})
z_0	Roelands z0 parameter
z_1	Roelands z1 parameter
θ_r	ref temp. in Roelands law (K)
θ_0	ref temp. for density and viscosity (K)
k	thermal conductivity coeff ($Wm^{-1}K^{-1}$)
k_a, k_b	thermal con. coeff of A/B ($Wm^{-1}K^{-1}$)

Reference Values

u_0	reference velocity (ms^{-1})
η_x	ambient viscosity (Nm^{-1})
ρ_x	ambient density (Nm^{-1})
θ_x	ambient temperature (K)

Non-Dimensional Values

B	Hertzian radius	($B = 2b/R$)
H	film thickness	($H = Rh/b^2$)
P	pressure	($P = p/p_h$)
T	time	($T = u_0t/2b$)
X	distance	($X = x/b$)
U_a	velocity of roller A	($U_a = u_a/u_0$)
U_b	velocity of roller B	($U_b = u_b/u_0$)
U_e	entrainment velocity	($U_e = u_e/u_0$)
U_m	mean velocity	($U_m = u_m/u_0$)
$\overline{\rho}$	density	($\overline{\rho} = \rho/\rho_x$)
$\overline{\eta}$	viscosity	($\overline{\eta} = \eta/\eta_x$)
$\overline{\theta}$	temperature	($\overline{\theta} = \theta/\theta_x$)
Γ_m	mean shear rate	($\Gamma_m = \lvert U_b - U_a\rvert/H$)

3. Governing Equations

There are five governing equations for the standard non-thermal line contact EHL problem, those of pressure, film thickness, force balance, density and viscosity. In addition there are three equations linked with the thermal model, these being the energy equation and a surface temperature equation for each surface.

The pressure distribution is modelled by the Reynolds Equation [17]. In non-dimensional form this is:

$$\frac{\partial(\overline{\rho}H)}{\partial T} = \frac{\partial}{\partial X}\left(\frac{\overline{\rho}H^3}{\overline{\eta}\lambda}\frac{\partial P}{\partial X}\right) - U_e(T)\frac{\partial(\overline{\rho}H)}{\partial X}, \quad (1)$$

where

$$U_e(T) = U_a(T) + U_b(T), \quad (2)$$

and

$$\lambda = \frac{6\eta_x u_e R^2}{b^3 p_h}. \quad (3)$$

The Film Thickness Equation represents the geometry of the roller and is given, in non-dimensional form, by:

$$\begin{aligned} H(X) &= H_0 + \frac{X^2}{2} \\ &\quad -\frac{1}{\pi}\int_{X_a}^{X_b} \ln|X - X'|P(X')\mathrm{d}X', \end{aligned} \quad (4)$$

where H_{00} is the central offset film thickness, which defines the relative positions of the surfaces if no deformation was to occur. The parabolic term represents the undeformed shape of the rollers, and the integral defines the deformation of the surface due to the pressure distribution across the domain.

The Force Balance Equation relates the pressure distribution across the domain to the applied load. It is given by:

$$\int_{-\infty}^{\infty} P(X)\mathrm{d}X = \frac{\pi}{2}. \quad (5)$$

The density of the fluid is normally modelled as a function of pressure only using the Dowson and Higginson [18] model. In this work we consider the density as being a function of both pressure and temperature and use an extended form of the Dowson and Higginson model in dimensional form:

$$\rho(p,\theta) = \rho_0\left(1+\frac{\mu p}{1+\nu p}\right)\{1-\beta_e(p)(\theta-\theta_0)\}, \quad (6)$$

where

$$\beta_e(p) = \beta_{e;0}\exp(-\kappa_e p). \quad (7)$$

Similarly to the density, in this work the viscosity is considered to be a function of both pressure and of temperature, instead of merely pressure. As a result the viscosity model used is a modified version of the Roelands law [19], this is:

$$\eta(p,\theta,\dot{\gamma}) = \eta_0\exp(y), \quad (8)$$

where

$$y = \frac{\alpha_0 p_0}{z_0}\left\{\left(1+\frac{p}{p_0}\right)^{z(\theta)}\left(\frac{\theta-\theta_r}{\theta_0-\theta_r}\right)^{-s}-1\right\}, \quad (9)$$

$$z(\theta) = z_0 - z_1\ln\left(\frac{\theta-\theta_r}{\theta_0-\theta_r}\right), \quad (10)$$

and

$$s = \frac{\beta_0 z_0}{\alpha_0 p_0}(\theta_0-\theta_r). \quad (11)$$

Temperature varies not only in the direction of flow through the contact which is solved for but also in the direction across the flow, between the rollers which is not solved for. Consequently an approximation must be made to take this into account. We assume a parabolic temperature approximation [15].

The appropriate Energy Equation for EHL problems [16] assuming the parabolic temperature approximation is given in non-dimensional form as:

$$\overline{\rho}\left\{\frac{1}{2}\frac{\partial\overline{\theta}}{\partial T}+U_m\frac{\partial\overline{\theta}}{\partial X}+\frac{(\overline{\theta}-\overline{\theta_b})(U_m-U_b)}{H}\frac{\partial H}{\partial X}\right\}$$
$$=\frac{3\overline{k}}{2B^2H^2}(\overline{\theta_a}+\overline{\theta_b}-2\overline{\theta})+\overline{\beta_e\theta}\left(\frac{1}{2}\frac{\partial P}{\partial T}+U_m\frac{\partial P}{\partial X}\right)$$
$$-2B\overline{\mu}\left(U_m-\frac{U_e}{2}\right)\frac{\partial P}{\partial X}+\frac{B\overline{\mu\kappa}}{3}\overline{\eta}\Gamma_m^2, \quad (12)$$

where

$$U_m = -\frac{H^2}{2\overline{\kappa\eta}}\frac{\partial P}{\partial X}+\frac{U_e}{2}, \quad (13)$$

$$\overline{\mu} = \frac{p_h R}{C_p\rho_x\theta_x b}, \quad (14)$$

$$\overline{\kappa} = \frac{6\eta_x u_r R^2}{b^3 p_h}, \quad (15)$$

$$\overline{\beta_e} = \frac{p_h\beta_e}{C_p\rho_x}, \quad (16)$$

and

$$\overline{k} = \frac{k}{C_p\rho_x u_0 b}. \quad (17)$$

The term on the left is heat convection, while the terms on the right of the equation model thermal conductivity, compression heating, viscous heat generation due to Pouseille flow and viscous heat generation due to Couette flow.

There are two equations for surface temperature, one for each surface. In the pure rolling case, these will be identical. The equations are given in non-dimensional terms as:

$$\overline{\theta_a(X)} = 1+2\frac{\overline{\kappa\chi_a}}{\sqrt{U_a}}\int_{-\infty}^{X}\frac{(3\overline{\theta}-2\overline{\theta_a}-\overline{\theta_b})}{(X-\overline{\zeta})^{1/2}H(X)}\mathrm{d}\overline{\zeta}, \quad (18)$$

and

$$\overline{\theta_b(X)} = 1+2\frac{\overline{\kappa\chi_b}}{\sqrt{U_b}}\int_{-\infty}^{X}\frac{(3\overline{\theta}-\overline{\theta_a}-2\overline{\theta_b})}{(X-\overline{\zeta})^{1/2}H(X)}\mathrm{d}\overline{\zeta}, \quad (19)$$

where

$$\overline{\upsilon} = \frac{b^3 p_h}{12R^2\eta_x\nu}, \quad (20)$$

$$\overline{\kappa} = \frac{k}{\rho_0 C_p\nu b}, \quad (21)$$

$$\overline{\nu} = \frac{6R^2}{b^2}, \quad (22)$$

$$\overline{\chi_a} = \frac{\rho_0 C_p\nu R}{\sqrt{\pi\rho_a C_{p:a}k_a u_0 b}}, \quad (23)$$

$$\overline{\chi_b} = \frac{\rho_0 C_p\nu R}{\sqrt{\pi\rho_b C_{p:b}k_b u_0 b}}. \quad (24)$$

Extension for Point Contact

The equations for the isothermal point contact model are well documented. After non-dimensionalisation, additional y-directional terms occur in the Reynolds equations, the force balance equation is altered and there are changes to the integral in the film thickness equation. The density and viscosity equations remain unchanged.

The Reynolds equation (1) becomes,

$$\begin{aligned}\frac{\partial(\overline{\rho}H)}{\partial T} &= \frac{\partial}{\partial X}\left(\frac{\overline{\rho}H^3}{\overline{\eta}\lambda}\frac{\partial P}{\partial X}\right) \\ &\quad + \frac{\partial}{\partial Y}\left(\frac{\overline{\rho}H^3}{\overline{\eta}\lambda}\frac{\partial P}{\partial Y}\right) - \frac{U_e(T)}{U_e(0)}\frac{\partial(\overline{\rho}H)}{\partial X},\end{aligned} \tag{25}$$

The Force Balance equation in the point contact case is given by:

$$\int_{-\infty}^{\infty}\int_{-\infty}^{\infty} P(X,Y)\mathrm{d}X\mathrm{d}Y = \frac{2\pi}{3}. \tag{26}$$

The film thickness equation is given by,

$$\begin{aligned}H(X,Y) &= H_{00} + \frac{X^2}{2} + \frac{Y^2}{2} \\ &-\frac{2}{\pi^2}\int_{-\infty}^{\infty}\int_{-\infty}^{\infty}\frac{P(X',Y')\mathrm{d}X'\mathrm{d}Y'}{\sqrt{(X-X')^2+(Y-Y')^2}},\end{aligned} \tag{27}$$

The mean energy equation has extra terms in the two dimensional case. The two-dimensional form of this equation is given by,

$$\begin{aligned}&\overline{\rho}\left\{\frac{1}{2}\frac{\partial\overline{\theta}}{\partial T} + U_m\frac{\partial\overline{\theta}}{\partial X} + V_m\frac{\partial\overline{\theta}}{\partial Y}\right. \\ &\left. + \frac{\overline{\theta}-\overline{\theta_b}}{H}\left((U_m-U_b)\frac{\partial H}{\partial X} + V_m\frac{\partial H}{\partial Y}\right)\right\} = \\ &\frac{3k}{2B^2H^2}(\overline{\theta_a}+\overline{\theta_b}-2\overline{\theta}) + \frac{B\overline{\mu}\kappa}{3}\overline{\eta}\Gamma_m^2 \\ &+\overline{\beta_e\theta}\left(\frac{1}{2}\frac{\partial P}{\partial T} + U_m\frac{\partial P}{\partial X} + V_m\frac{\partial P}{\partial Y}\right) \\ &-2B\overline{\mu}\left\{\left(U_m - \frac{U_e}{2}\right)\frac{\partial P}{\partial X} - V_m\frac{\partial P}{\partial Y}\right\},\end{aligned} \tag{28}$$

where

$$V_m = -\frac{H^2}{2\kappa\overline{\eta}}\frac{\partial P}{\partial Y}. \tag{29}$$

4. Discretisation

A uniform mesh is used with N elements where $N = 2^k + 1$. The level of refinement on a grid can then be described as grid level k refinement. The equations are discretised using first order upwind differencing, or second order central differencing where appropriate. This discretisation has been documented elsewhere [20] for the non thermal equations, so here we shall only consider the energy and two surface temperature equations.

The Energy Equation (12) is discretised as:

$$\begin{aligned}&\overline{\rho_i}\left\{\frac{(\overline{\theta_i^{t_n}}-\overline{\theta_i^{t_{n-1}}})}{2\Delta T} + U_m\frac{(\overline{\theta_i}-\overline{\theta_{i-1}})}{\Delta X}\right. \\ &\left. + \frac{(\overline{\theta_i}-\overline{\theta_b})}{H}\left((U_m-U_b)\frac{H_i-H_{i-1}}{\Delta X}\right)\right\} = \\ &\frac{3k}{2B^2H_i^2}(\overline{\theta_a}+\overline{\theta_b}-2\overline{\theta_i}) + \\ &\overline{\beta_e\theta_i}\left(\frac{(P_i^{t_n}-P_{i-1}^{t_{n-1}})}{2\Delta T} + U_m\frac{(P_i-P_{i-1})}{\Delta X}\right) - \\ &2B\overline{\mu}\left(U_m-\frac{U_e}{2}\right)\frac{(P_i-P_{i-1})}{\Delta X} + \frac{B\overline{\mu}\kappa}{3}\overline{\eta}\Gamma_m^2,\end{aligned} \tag{30}$$

where,

$$U_m = -\frac{H_i^2}{2\kappa\overline{\eta}}\frac{(P_i-P_{i-1})}{\Delta X} + \frac{U_e}{2}. \tag{31}$$

The Surface Temperature Equations (18) and (19) become:

$$\begin{aligned}\overline{\theta_{a;i}} &= 1 + 2\overline{\kappa\chi_a}\sum_{j=1}^{i}\left\{\frac{\overline{\theta_{A;j-1}}+\overline{\theta_{A;j}}}{H_{j-1}+H_j}\right. \\ &\quad \left. 2\{(X_j-X_{j-1})^{1/2}-(X_i-X_j)^{1/2}\}\right\},\end{aligned} \tag{32}$$

and

$$\begin{aligned}\overline{\theta_{b;i}} &= 1 + 2\overline{\kappa\chi_b}\sum_{j=1}^{i}\left\{\frac{\overline{\theta_{B;j-1}}+\overline{\theta_{B;j}}}{H_{j-1}+H_j}\right. \\ &\quad \left. 2\{(X_j-X_{j-1})^{1/2}-(X_i-X_j)^{1/2}\}\right\},\end{aligned} \tag{33}$$

where,

$$\overline{\theta_A} = 3\overline{\theta} - 2\overline{\theta_a} - \overline{\theta_b}, \tag{34}$$

and

$$\overline{\theta_B} = 3\overline{\theta} - \overline{\theta_a} - 2\overline{\theta_b}. \tag{35}$$

5. Solution Method

The equations, excluding the thermal equations, are solved using multigrid techniques in in the standard manner as described in [21,20,22] and utilising the multilevel multi-integration algorithm of Brandt and Lubrecht [23].

The temperature, both at the surface and in the fluid is calculated only on the finest mesh. First the surface temperatures are calculated using equations (32) and (33). This can be an expensive process as at each point a summation along the line up to that point is required. Furthermore the calculation at each point is expensive when repeated. Following the surface calculation, the Energy Equation (30) is calculated at each point using a Newton method. The relaxation factor is initially small but can be allowed to increase once the solution is converging.

In the multigrid method the temperature is also required on the coarser grids. This is obtained by coarsening the temperature on the fine mesh, no temperature solve being carried out on these meshes.

6. Results

Moes Parameter M	27.68
Moes Parameter L	9.53
Speed Parameter U	1.6×10^{-11}
Material Parameter G	4000
Load Parameter W	1.57×10^{-4}
Pressure-viscosity index α	2.0×10^{-8} Pa^{-1}
Maximum Hertzian Pressure p_h	1.0×10^{9} Pa
Minimum Domain Bound	-4.6×10^{-3} m
Maximum Domain Bound	4.6×10^{-3} m
Number of Points	2049

Table 1
Operating Parameters for Line Contact Case

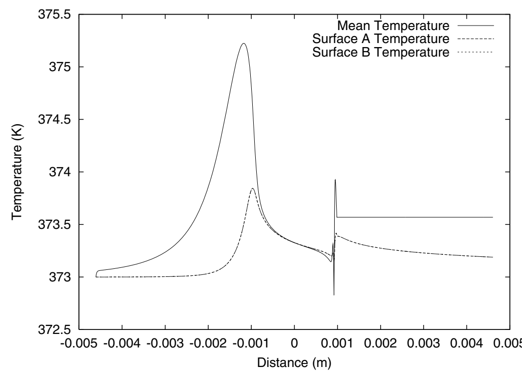

Figure 1. Temperature Profile in Pure Rolling Case

6.1. Steady State Line Contact

Figure 1 shows the mean fluid and surface temperature profiles for a pure rolling case, as described in Table 1, with both rollers always travelling with an identical velocity of $3.0ms^{-1}$. The mean temperature can be seen to smoothly rise to a peak upstream of the contact region, before rapidly decreasing as the contact region is entered. The temperature then slowly decreases across the contact region until a spike coinciding with the exit of the contact region. The surface temperature follows the same profile but at a lower temperature and translated slightly further downstream than the mean temperature profile.

If small amounts of shear occur then very different solution profiles are obtained. Figure 2 shows three mean fluid temperature solutions, the first solution is for pure rolling and the subsequent two are with slight amounts of shear. The structure of the pure rolling profile can barely be made out as the rise in temperature in the middle of the contact region is so large. The shear profile does exhibit these features but they remain of the same size as in the rolling case.

6.2. Transient Line Contact

The behaviour of the model in Table 1 under transient conditions is investigated using a reversal case. Each roller at $t = 0$ has a velocity and over a time period this is gradually changed until

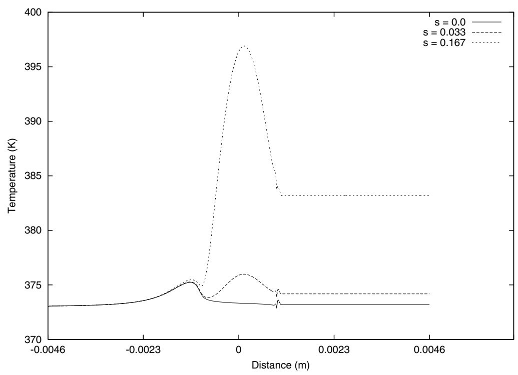

Figure 2. Temperature Profile in Shear Cases

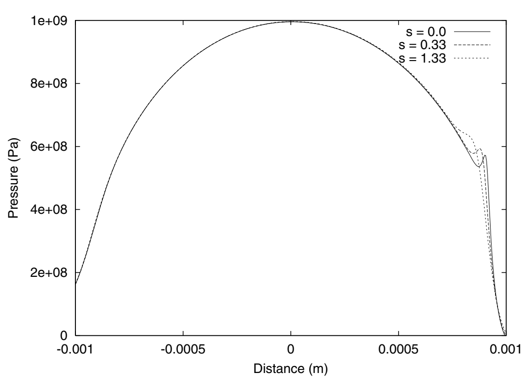

Figure 3. Pressure Profile in Shear Cases

finally it is travelling at the opposite velocity.

In the first case pure rolling is considered with both rollers always travelling at identical velocities to each other. Initially they are travelling at 3.0ms^{-1} and decrease linearly over a period of 0.2s to a final velocity of -3.0ms^{-1}. There are 500 timesteps of 0.0004s taken.

In the second and third cases shear is introduced, at a low level and at a high level. The second model has the rollers initially with velocities of 2.5ms^{-1} for Roller A and 3.5ms^{-1} for Roller B, the third with velocities of 1.0ms^{-1} for Roller A and 5.0ms^{-1} for Roller B. In both cases these velocities vary linearly with time over a period of 0.2s to final opposite velocities. There are 500 timesteps of 0.0004s taken.

Figures 4 show the temperature profiles for all three cases at 5 points during the reversal run. As can be seen the temperature of the model with the largest shear dominates the profiles displaying a maximum rise in excess of 100 degrees. This decreases as the velocity is reduced and at the point of reversal the temperature has reduced to ambient throughout the domain.

A similar effect can be seen with the temperatures at the surface of the roller. Figures 5 show the surface temperatures on the two rollers. The temperature profile on each roller is clearly the same as for the other roller, but at different values. Roller A, the slower of the two rollers clearly has lower temperature profiles than the faster roller.

7. Steady Point Contact

Figure 6 shows two mean fluid temperature solutions in the point contact case with operating parameters detailed in Table 2. The lower of the two solutions is for the pure rolling case, the higher solution is for a case with a small amount of shear. The pure rolling model has both rollers travelling with a velocity of 4.0ms^{-1}, the shear case has roller velocities of 4.01ms^{-1} and 3.99ms^{-1} giving a shear rate of $s = 0.005$. In the pure rolling solution the temperature can be seen to rise upstream of the contact region, falling to ambient within this region, before a spike at the exit of the contact region. The case with the shear

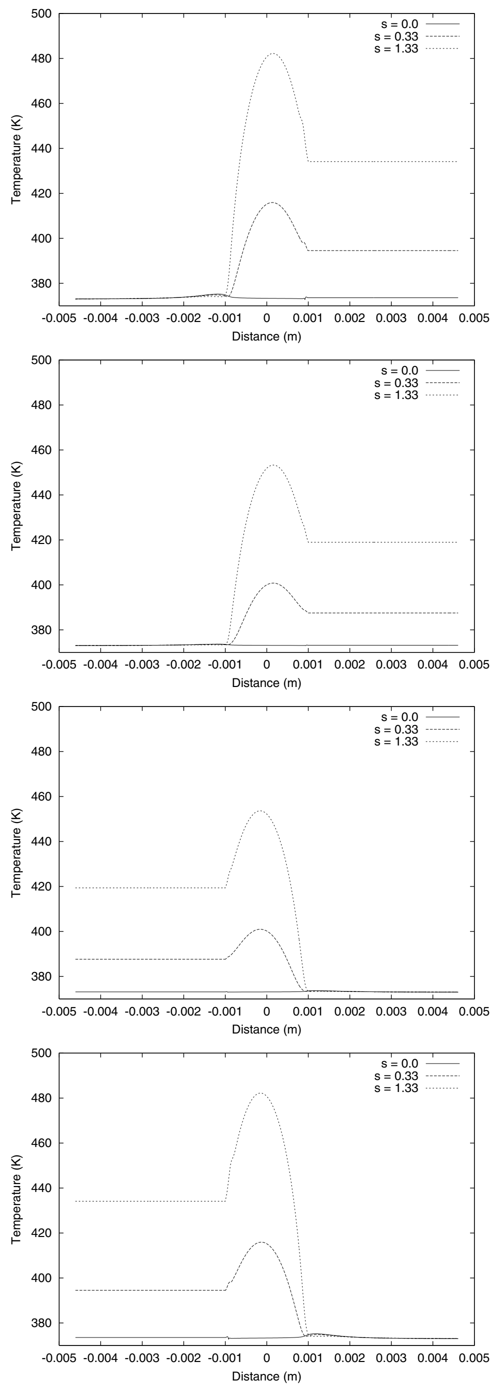

Figure 4. Mean Fluid Temperature Profiles at t=0.0s,0.05s,0.15s,0.20s

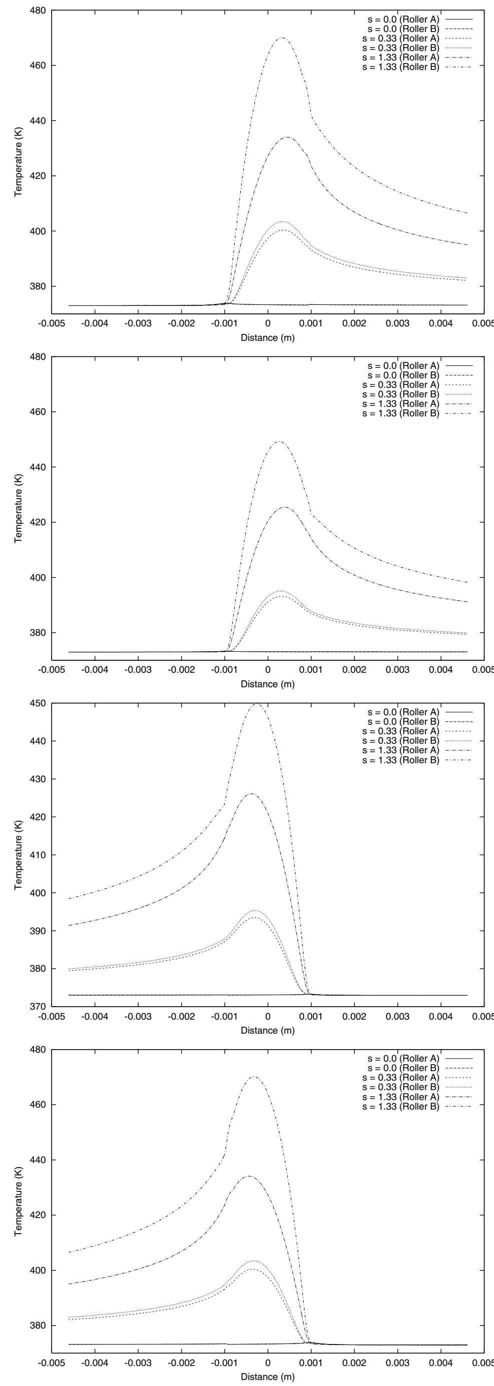

Figure 5. Surface Temperature Profiles at t=0.0s,0.05s,0.15s,0.20s

Moes Parameter M	33.38
Moes Parameter L	17.90
Speed Parameter U	1.6×10^{-10}
Material Parameter G	4200
Load Parameter W	2.58×10^{-6}
Pressure-viscosity index α	$2.1\times10^{-8}Pa^{-1}$
Maximum Hertzian Pressure p_h	$1.0\times10^{9}Pa$
Minimum Domain Bound	$-4.86\times10^{-3}m$
Maximum Domain Bound	$2.50\times10^{-3}m$
Number of Points	257×257

Table 2
Operating Parameters for Point Contact Case

displays the same features except that there is a large temperature rise in the centre of the contact region relative to the rolling case, the ambient temperature being $373K$ and the peak temperature $384K$.

8. Conclusions

It has been shown that an energy equation can be successfully incorporated into the EHL solver of [14] to obtain mean and surface temperature solutions for both steady state and transient cases. The importance of shear in an EHL contact has also been demonstrated with even small amounts of shear producing temperatures far in excess of those found within the contact under pure rolling conditions. This increase in temperature can also be seen to influence the spike in the pressure profile.

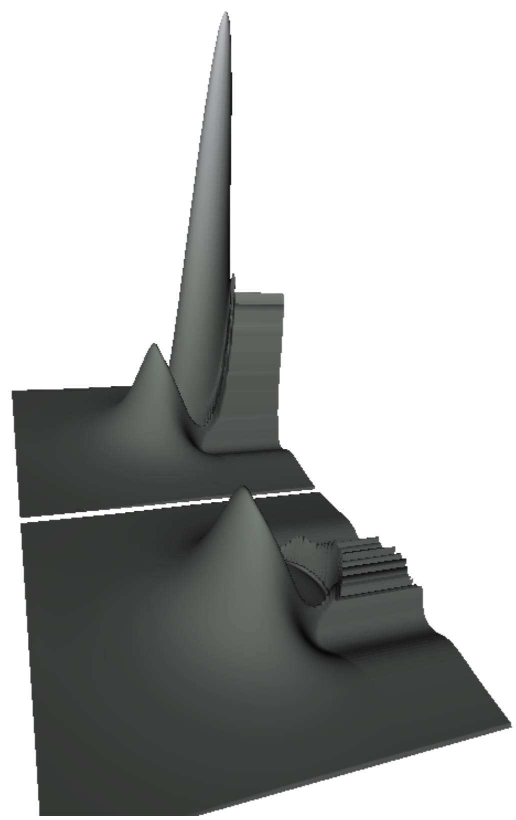

Figure 6. Mean Fluid Temperature Profiles

REFERENCES

1. Ausherman, V.K., Nagaraj, H.S., Sanborn, D.M. and Winer, W.O., Infrared temperature mapping in elastohydrodynamic lubrication, *Trans. ASME, Journal of Tribology*, 1993, 115, 102-110.
2. Crook, A.W., The lubrication of rollers. Part III., *Phil. Trans. R. Soc. Lond. A*, 1961, 83, 213-226.

3. Sternlicht, B., Lewis, P. and Flynn, P., Theory of lubrication and failure of rolling contacts, *ASME J.Basic Eng*, 1961, 83, 213-226.
4. Cheng, H.S and Sternlicht, B., A numerical solution for the pressure, temperature and film thickness between two infinitely long, lubricated rolling and sliding cylinders, under heavy loads, *Trans. ASME, J.Basic Eng*, 1965, 103, 695-707.
5. Cheng, H.S., A refined solution to the thermal-elastohydrodynamic lubrication of rolling and sliding cylinders, *ASLE Trans.*, 1965, 8, 397-410.
6. Dowson, D. and Whitaker, A.V., A numerical procedure for the solution of the elastohydrodynamic problem of rolling and sliding contacts lubricated by a Newtonian fluid, *Proc. Inst. Mech. Eng.*, 1965, 180, 57-71.
7. Lee, R.T. and Hsu, C.H., Advanced multilevel solution for thermal elastohydrodynamic lubrication of simple sliding line contacts, *Wear*, 1994, 171, 227-237.
8. Lee, R.T. and Hsu, C.H., Multilevel solution for thermal elastohydrodynamic lubrication of rolling/sliding circular contacts, *Tribology International*, 1995, 28(8), 541-552.
9. Kim, H.J., Ehret, P., Dowson, D. and Taylor, C.M., Thermal elastohydrodynamic analysis of circular contacts. Part 1: Newtonian model, *Proc Instn Mech Engrs, Part J, J. of Engineering Tribology*, 2001, 215, 339-352.
10. Kim, H.J., Ehret, P., Dowson, D. and Taylor, C.M., Thermal elastohydrodynamic analysis of circular contacts. Part 2: non-Newtonian model, *Proc Instn Mech Engrs, Part J, J. of Engineering Tribology*, 2001, 215, 353-362.
11. Kazama, T., Ehret, P. and Taylor, C.M., On the effects of the temperature profile approximation in thermal Newtonian solutions of elastoydrodynamic lubrication line contacts, *Proc Instn Mech Engrs, Part J, J. of Engineering Tribology*, 2001, 215(J1), 109-120.
12. Venner, C.H. and Lubrecht, A.A., Multilevel methods in lubrication, *Tribology Series, 37*, ed D.Dowson, Elsevier, 2000.
13. Nurgat, E., Berzins, M. and Scales, L., Solving EHL problems using iterative, multigrid, and homotopy methods, *Trans. ASME, J. Tribology*, 1999, 121(1), 28-34.
14. Goodyer, C.E., Fairlie, R., Berzins, M. and Scales, L.E., Adaptive techniques for elastohydrodynamic lubrication solvers, *Tribology Research : From Model Experiment to Industrial Problem, Proceedings of the 27th Leeds-Lyon Symposium on Tribology*, ed G.Dalmaz et al, Elsevier, 2001.
15. Salehizadeh, H. and Saka, N., Thermal non-Newtonian elastohydrodynamic lubrication of rolling line contacts, *Trans. ASME, J. Tribology*, 1991, 113, 481-491.
16. Scales, L.E., Quantifying the Rheological Basis of Traction Fluid Performance, *SAE Technical Paper Series*, No.1999-01-3610, 1999.
17. Reynolds, O., On the theory of lubrication and its application to Mr Beauchamp Tower's experiments, including an experimental determination of the viscosity of olive oil, *Philosophical Transactions of the Royal Society of London*, 1886, 177, 157-234.
18. Dowson, D. and Higginson, G.R., Elastohydrodynamic Lubrication, The Fundamentals of Roller and Gear Lubrication., Permagon Press, Oxford, Great Britain, 1966.
19. Roelands, C.J.A., Correlational Aspects if the viscosity-temperature-pressure relationship of lubricating oils., *PhD thesis*, Technische Hogeschool Delft, The Netherlands, 1966.
20. Goodyer, C.E., Elastohydrodynamic Lubrication, *PhD thesis*, University of Leeds, Leeds, England, 2002.
21. Venner, C.H., Multilevel Solution of the EHL Line and Point Contact Problems, *PhD thesis*, University of Twente, The Netherlands, 1991.
22. Goodyer, C.E., Fairlie, R., Berzins, M. and Scales, L.E., An in-depth investigation of the multigrid approach for steady and transient EHL problems, *Thinning films and Tribological Interfaces: Proceedings of the 26th Leeds-Lyon Symposium on Tribology*, ed D.Dowson et al, Elsevier, 2000.
23. Brandt, A. and Lubrecht, A.A., Multilevel matrix multiplication and fast solution of integral equations, *Journal of Computational Physics*, 1990, 90(2), 348-370.